EFFECT OF LASER FLUENCE ON THE CHARACTERISTICS OF GRAPHENE NANOSHEETS PRODUCED BY PULSED LASER ABLATION IN WATER

Samaneh Kamali [1], Elmira Solati [2], Davoud Dorranian [3*]

[1] Islamic Azad University, Central Tehran Branch, Physics Department, Science Faculty, Tehran, Iran
[2] Young Researchers and Elite Club, Science and Research Branch, Islamic Azad University, Tehran, Iran
[3] Plasma Physics Research Center, Science and Research Branch, Islamic Azad University, Tehran, Iran; e-mail: doran@srbiau.ac.ir

The effect of laser fluence on the characteristics of carbon nanostructures produced by pulsed laser ablation has been investigated. The beam of a Q-switched Nd:YAG laser of 1064 nm wavelength at 7 ns pulse width and different fluences was employed to irradiate the graphite target in distilled water. The X-ray diffraction pattern, transmission electron microscopy, field emission scanning electron microscopy, Raman spectrum, and linear absorption properties of carbon nanostructures were used to characterize the ablation products. Carbon nanoparticles beside the graphene nanosheets were observed due to variation of laser fluence. The results show that under our experimental condition with increasing laser fluence the amount of carbon nanoparticles in suspensions was increased while the amount of graphene nanosheets was decreased.

Keywords: *graphite, graphene nanosheet, pulsed laser ablation, carbon nanoparticle.*

ВЛИЯНИЕ ПЛОТНОСТИ ЛАЗЕРНОГО ИЗЛУЧЕНИЯ НА ХАРАКТЕРИСТИКИ НАНОСЛОЕВ ГРАФЕНА, ПОЛУЧЕННЫХ ПРИ ИМПУЛЬСНОЙ ЛАЗЕРНОЙ АБЛЯЦИИ В ВОДЕ

S. Kamali [1], E. Solati [2], D. Dorranian [3*]

УДК 621.373.8;620.3

[1] Исламский университет Азад, Центральный тегеранский филиал, Тегеран, Иран
[2] Клуб молодых исследователей и элиты, Исламский университет Азад, Тегеран, Иран
[3] Научно-исследовательский центр физики плазмы, Исламский университет Азад, Тегеран, Иран; e-mail: doran@srbiau.ac.ir

(Поступила 6 марта 2018)

Исследовано влияние плотности лазерного излучения на характеристики углеродных наноструктур, получаемых импульсной лазерной абляцией. Для этого графитовая мишень в дистиллированной воде облучалась импульсами YAG:Nd-лазера с модуляцией добротности при ширине импульса 7 нс и различной плотности потока лазерного излучения на λ = 1064 нм. Для получения характеристик продуктов абляции использованы рентгеновская дифракция, просвечивающая электронная микроскопия, полевая эмиссионная сканирующая электронная микроскопия, спектры комбинационного рассеяния и характеристики линейного поглощения углеродных наноструктур. При изменении плотности лазерного излучения наряду с нанослоями графена наблюдались наночастицы углерода. В данных экспериментальных условиях при увеличении плотности лазерного излучения количество углеродных наночастиц в суспензиях увеличивалось, а количество нанослоев графена уменьшалось.

Ключевые слова: *графит, нанослой графена, импульсная лазерная абляция, углеродная наночастица.*

Introduction. Graphene is composed of a single layer of carbon atoms formed in a honeycomb lattice. It has attracted lots of attention since it was discovered experimentally in 2004. Graphene is a two-dimensional carbon material with sp^2 bonds and has relativistic energy dispersion [1, 2]. The considerable interest in graphene can be due to three reasons. First, its electron transport may be defined by the Dirac equation and this allows one to approach quantum electrodynamics in a simple condensed matter experiment [3, 4]. Second, the scalability of graphene to nanoscale dimensions [5] makes it an attractive candidate for applications, due to its ballistic transport at room temperature combined with chemical and mechanical stability. Third, various forms of graphite, nanotubes, and others can be considered as derivatives of graphene [6].

Different techniques, including chemical or physical methods, have been used to produce the carbon nanostructures [7]. Among the various techniques, the pulsed laser ablation (PLA) method has attracted a lot of attention in the production of materials on the nano-scale [8–10]. There are many advantages for the synthesis of nanostructured materials from a solid target in a liquid medium by the PLA method. The first advantage of the PLA method is the low-cost equipment for controlling the ablation atmosphere. Another important feature of the PLA method is the high purity of products without any contamination and side products [11, 12]. Most importantly, it has been shown that the size, morphology, and structure of the synthesized material can be controlled by varying parameters such as laser wavelength, laser fluence [9], laser pulse width [10], aqueous ablation environment [13, 14], and temperature of liquid environment [15, 16].

Experimental work on the production of carbon nanostructures by the PLA method has been carried out. In 2012, Mortazavi et al. prepared the graphene layer by pulsed laser ablation of a graphite target inside liquid nitrogen [17]. Chen et al. in 2007 [18] synthesized the carbon nanoparticles an different solutions using the PLA method. In their work, carbon nanoparticles synthesized in water are slightly larger than those made in tetrahydrofuran. Carbon nanoparticles produced in both liquids have an amorphous phase and cover a wide range of wavelengths with high transmittance [18]. Recently, we showed the effects of the volumetric ratio zinc oxide and graphene suspensions on the nonlinear response of a mixture of ZnO nanoparticles and graphene nanoparticles produced by the PLA method [19]. Tabatabaie et al. reported on the effect of laser fluence on the production of graphene nanosheets by pulsed laser ablation in liquid nitrogen [20].

In this work, we have used distilled water as the ablation environment, and the effect of the laser fluence on the production of carbon nanostructures such as graphene nanosheets and carbon nanoparticles by the PLA method has been investigated experimentally.

Experimental set up. Carbon nanostructures such as graphene nanosheets were produced by pulsed laser ablation of a graphite target (99.99%) placed at the bottom of a glass vessel filled with 80 ml distilled water. Before ablation, the graphite target and containers were cleaned ultrasonically in alcohol, acetone, and distilled water for 10 min respectively. The graphite target was irradiated vertically with the first harmonic of a Q-switched Nd:YAG laser (λ = 1064 nm) of 7 ns pulse width and 5 Hz repetition rate. Each sample was prepared with 5000 laser pulses. Samples 1–5 were prepared with a laser fluence of 0.5, 0.7, 1, 1.2, and 1.5 J/cm^2, respectively. A convex lens with its focal length of 80 mm was used to focus the laser beam on the surface of graphite target in water. The height of water on the target was 5 mm during the ablation.

A variety of analytical techniques was applied for characterization of products. Optical absorption spectra of the samples in a quartz cell of 10 mm path length were measured by an UV-Vis-NIR spectrophotometer from PG Instruments (T-80). A Zeiss-EM10C-80kV transmission electron microscope (TEM) and a Hitachi S4160 field emission scanning electron microscope (FE-SEM) were employed for taking the images of the samples at different scales. For TEM imaging, a few drops of suspensions were dried on a carbon coated copper grid and for FE-SEM imaging, a few drops of suspensions were dried on a silicon substrate. The X-ray diffraction (XRD) pattern of the dried drops of suspension on the silicon substrate was measured using a STOE-XRD system. A Raman thermonicolet disperse spectroscope from Almega was utilized to determine the structure, quality, and amount of graphene in the dried drops of suspensions on the glass substrate. The molecular structures of the samples were characterized by a Nexus 870 Fourier transform infrared (FTIR) spectroscope.

Results and discussion. UV-Vis-NIR absorption spectra, FTIR spectra, and XRD analyses were carried out to examine the optical properties and crystal structures of carbon nanostructures such as graphene nanosheets and carbon nanoparticles (Fig. 1). Suspensions of the carbon nanostructures contain carbon nanosheets, i.e., graphene and carbon nanoparticles. With increasing laser fluence the color of the samples was changed from colorless to dark brown. In this case the color of the suspension may depend on the carbon nanostructure size, concentration, and morphology. The color of carbon nanostructures in sample 4 and 5 is darker than the other samples, which can be due to the larger concentration of carbon nanoparticles in these

solutions. In this experiment with increasing laser fluence, the amount of graphene nanosheets in the suspensions decreases. It is clear that the size of nanostructure and properties of carbon nanostructures produced by laser ablation are strongly dependent on the experimental parameters such as laser fluence.

The absorption spectra of the samples are shown in Fig. 1a. UV-Vis-NIR absorption spectra were obtained in order to characterize the optical absorbance of the colloidal solutions and to confirm the nature of the carbon nanostructures. The spectra were recorded with distilled water as the baseline reference in a 1 cm thickness quartz cell. The typical UV-Vis-NIR absorption spectrum of suspensions of carbon nanostructures shows a plasmonic peak around 300 nm due to n–π^* transitions of C=O [21, 22]. The characteristic feature of graphene can be due to the appearance of an absorption peak at about 300 nm in oxidized graphite. The intensity of the absorption peak in the nanostructures of sample 4 and 5 is higher than in the other samples and is due to a larger number of carbon nanoparticles in these samples. This result is confirmed by the color of the carbon nanostructure suspensions. A lighter color of the solution represents a lower concentration of carbon nanoparticles, whereas a darker color indicates a higher concentration of carbon nanoparticles. The intensity of the absorption peak for the carbon nanostructure confirms that the number of carbon nanoparticles produced at higher fluence is greater than at other fluences. In the other words, the concentration of the graphene nanosheets in solution increased with decreasing laser fluence.

FTIR spectra of the carbon nanostructure prepared by laser pulses in distilled water are shown in Fig. 1b. The FTIR spectrum was recorded in the spectral range of 400–4000 cm^{-1}. The peak at 700 cm^{-1} is due to a vinyl or aromatic C–H bond. These bonds may be formed between carbon atoms and hydrogen atoms of water medium. The absorption peak in the range of 3200–3600 cm^{-1} is correlated to the O–H stretch of H_2O molecules [8]. The peak in the range of 1630 to 1650 cm^{-1} shows the C=C bond [23]. The signal in the FTIR spectrum at 2075 cm^{-1} was in agreement with the reported value for carbon-carbon triple bonds (between 2000 and 2200 cm^{-1}) [24]. The intensity of an absorption band in FTIR spectra depends on the number of the specific bonds present. In this work, the intensity of absorption bands at 1630–1650, 2075, and 3200–3600 cm^{-1} in all samples increased with increasing laser fluence, but the intensity of the absorption band at 700 cm^{-1} is random in the samples.

XRD spectra of the samples are presented in Fig. 1c. The X-ray diffraction measurement was performed for dried films of the samples from the concentrated suspension on a Si substrate. A peak of X-ray photons diffracted from the Si substrate can be seen at $2\theta = 69.41^{\circ}$ and the XRD spectrum of the graphite target is plotted at the bottom of the Fig. 1c. The graphite target has a strong peak at $2\theta = 26.4°$ and two weak peaks at 44.4° and 55°, respectively. As can be seen, the preferred orientation of the lattice structure of the carbon

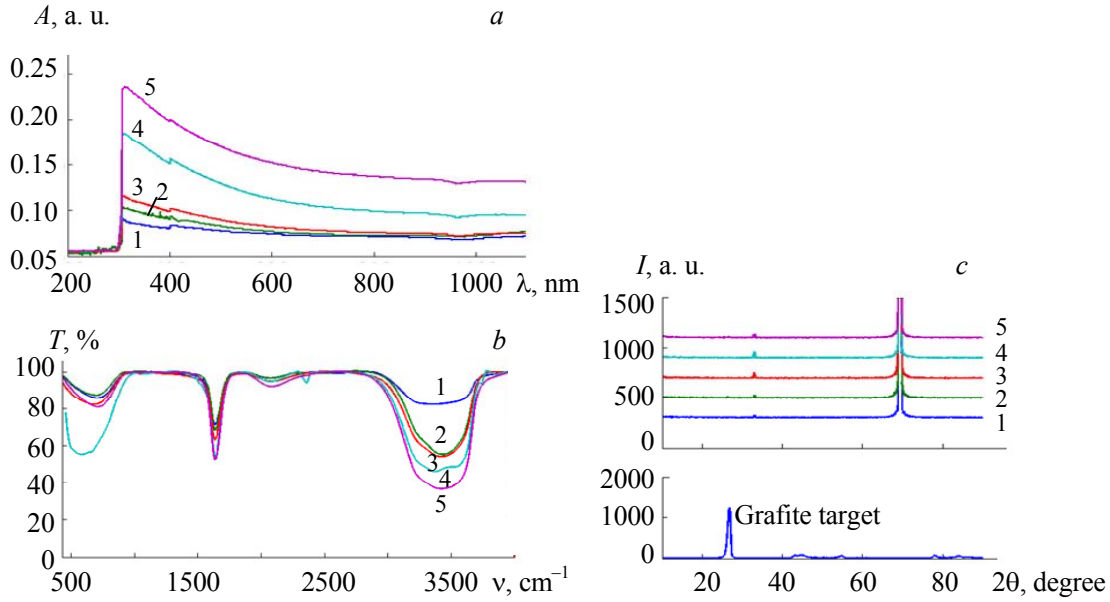

Fig. 1. UV-Vis-NIR absorption (a) and FTIR (b) spectrum of the samples 1–5, and XRD spectrum from the synthesized samples and graphite target (c).

nanostructure produced by pulsed laser ablation is completely different for the graphite target. A small peak at $2\theta = 33°$ is attributed to the structure of fullerite in the samples [25]. In fact, we do not expect any XRD peaks from the monolayer graphene. Generally, graphene as the two-dimensional material is not able to create resonance and XRD peaks, so the absence of strong XRD peaks in the samples is evidence of nanosheets in multilayer graphene in the samples. In this experiment the nanostructures produced with 0.5 and 0.7 J/cm^2 laser fluence should be close to the graphene structure because of their weak peak. This result is confirmed by TEM micrographs and UV-Vis-NIR absorption spectra of the samples. According to TEM micrographs, transparent graphene nanosheets are formed in samples 1 and 2. Due to the smaller amount of carbon nanoparticles in these samples, the intensity of the absorption peak in these samples (samples produced with 0.5 and 0.7 J/cm^2 laser fluence) is lower than in the other samples.

Figure 2a shows TEM micrographs of the samples. The TEM images show the existence of graphene nanosheets as well as a variety of carbon nanostructures. Graphene nanosheets represent the morphology of transparent sheets, and folding of graphene can be seen on the sheets. From the TEM results, it was found that the laser fluence was a parameter that affected the type of carbon nanostructure produced. In the sample 1 (produced with the lowest laser fluence) we observed the most transparent graphene nanosheets and the least number of nanoparticles. In the other samples, by increasing the laser fluence, graphene nanosheets become darker, and this result can be attributed to an increase in the number of graphene nanosheets. Also, the number of carbon nanoparticles increased with increase in laser fluence. These results are in good agreement with the absorption spectroscopy results.

Figure 2b illustrates the FE-SEM micrographs of the samples. In sample 1 a large number of graphene nanosheets with dimensions of microns and minimal thickness can be seen. In the second sample, there are less graphene nanosheets and they are thicker, and also in this case a number of points can be seen that are due to other carbon structure. According to FE-SEM images of samples 1 and 2, we have seen the best graphene nanosheets compared to other samples. In the other samples the number of graphene nanosheets decreased, and so the thickness of the graphene nanosheets increased, and they are completely darkened. Also in samples 3, 4, and 5 the number of other carbon structure increased. The results of FE-SEM images are in a good agreement with other results in our work.

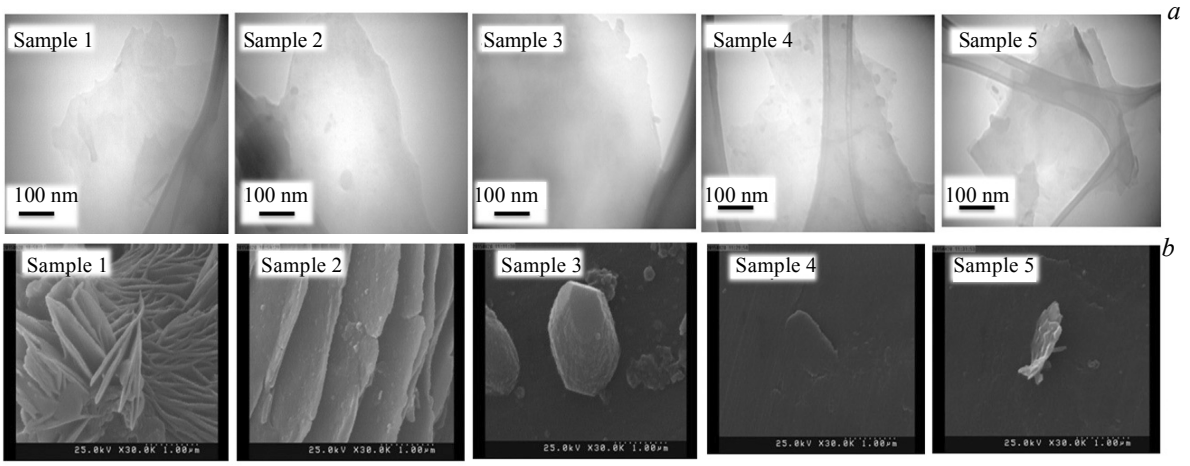

Fig. 2. TEM (a) and FE-SEM (b) micrographs of the carbon nanostructures.

Raman spectra of the samples are presented in Fig. 3. The data have been recorded with 0.1 cm^{-1} spectral resolution from the dried drops of suspensions on a glass substrate. The main features in the Raman spectra of carbons are the so called *G* and *D* peaks, which lie at 1200–1450 and 1500–1600 cm^{-1}, respectively, for visible excitation [17]. The assignment of the *D* and *G* peaks is straightforward in the "molecular" picture of carbon materials. These bands are present in all polyaromatic hydrocarbons. The *G* band is due to the bond stretching of all pairs of sp^2 atoms and points out the optical E_{2g} phonons at the Brillouin zone center. The *D* band is due to the breathing modes of sp^2 atoms in rings [26, 27].

As can be seen in Fig. 3a, the *D* and *G* lines are observed in the spectra at around 1360 and 1590 cm^{-1} corresponding to the generated graphene. With increasing local defects in the graphene, the *D* band intensity increases [19]. By comparing the intensity of the *D* and *G* bands in the samples, we see that we can achieve

the quality of the graphene produced in the samples. As we can see from the diagrams in Fig. 3a, the intensity of the *G* band for all samples is greater than the *D* band. This result shows that the quality of the graphene nanosheets in the samples is acceptable. At the same time, by increasing the laser pulse energy from 0.5 to 1.5 J/cm^2, the intensity of the *G* band decreased. In samples 1 and 2, the small magnitude of the ratio of the integrated intensity of the disorder-induced *D* band to that of *G* (I_D/I_G) indicates the increased fraction of sp^2 domains in these samples and suggests a satisfactory quality of the graphene nanosheets produced in lower laser fluence. Overall in this experiment, with increasing laser fluence the quality of graphene nanosheets is reduced. According to other result of the analyses the number of carbon nanoparticles increased with increasing laser fluence.

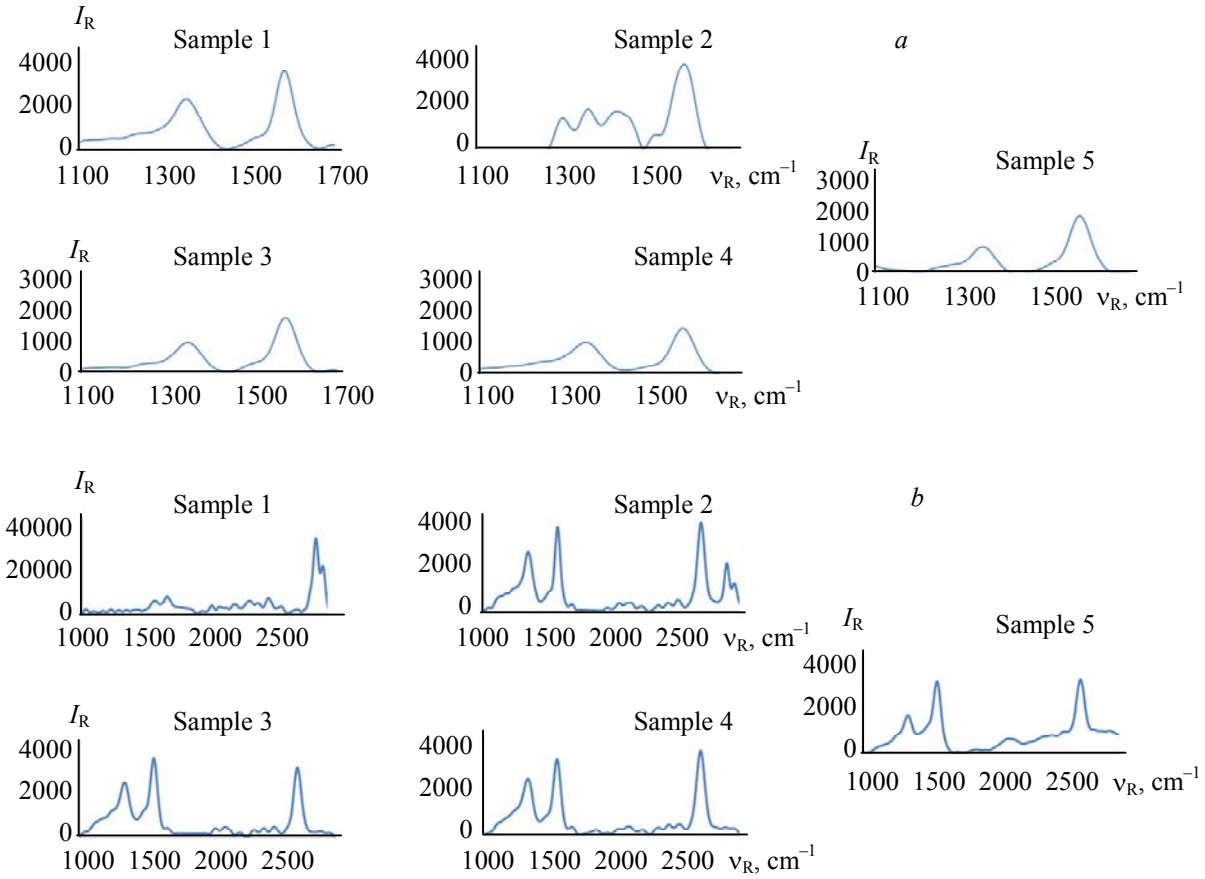

Fig. 3. Raman scattering spectrum of the samples (1–5) in the ranges of 1100–1700 (a) and 1000–3000 cm^{-1} (b).

The Raman shift spectra caused by the dried suspension of the carbon nanostructures in the range of 1000–3000 cm^{-1} are presented in Fig. 3b. A strong peak in the range of 2500–2800 cm^{-1} in the Raman spectra is due to the sp^2 carbon materials. This band in the Raman spectrum is a distinguishing feature of graphitic sp^2 materials and is called 2*D*-band. According to reports, the *2D*-band is a second-order two-phonon process, and the frequency is strongly dependent on the excitation laser energy [28]. Figure 4b shows that in the Raman spectra for samples 2–5 the 2*D*-band occurred around 2700 cm^{-1}. In sample 1, this peak is shifted towards higher frequencies. This shift may be due to the formation of graphene oxide in this sample [29]. The number of graphene layers is correlated to the feature of the peak in the 2*D*-band. When the layers of graphene increase, the Raman spectrum will be not the same for the monolayer graphene, which is due to the added forces from the interactions between layers of the AB-stacked graphene. In other words, the splitting of the peak in the 2*D*-band leads to an increasing number of modes that can combine to produce a wider, shorter, higher frequency peak [19, 20].

Conclusion. In this experiment, carbon nanostructures such as carbon nanoparticles and graphene nanosheets have been synthesized using pulsed nanosecond Q-switched Nd:YAG laser ablation of graphite in distilled water medium. TEM micrographs and data of other analyses, such as UV-Vis-NIR absorption spectra, confirm that the carbon nanostructures are divided into two classes of multilayer graphene and carbon nanoparticles. The results indicate that the amount of graphene nanosheets and the number of the carbon nanoparticles are proportional to laser fluence. According to the results, the amount of the carbon nanoparticles in the suspension increases with increasing laser fluence. The high intensity of the absorption peak in the sample produced with a laser fluence of 1.5 J/cm^2 confirms that the number of the carbon nanoparticles produced under this fluence is greater than under other fluences. In accordance with the TEM micrographs, the graphene nanosheets are more transparent in the samples produced with lower laser fluence. The FE-SEM micrographs show that in the sample produced with the laser fluence of 0.5 J/cm^2, a large number of graphene nanosheets with dimensions of microns and minimal thickness are formed. The Raman spectra show that a satisfactory quality of graphene nanosheets can be achieved in lower laser fluence.

REFERENCES

1. K. S. Novoselov, A. K. Geim, S. V. Morozov, D. Jiang, M. I. Katsnelson, I. V. Grigorieva, S. V. Dubonos, A. A. Firsov, *Nature*, **438**, 197–200 (2005).
2. Y. Zhang, Y. W. Tan, H. L. Stormer, P. Kim, *Nature*, **438**, 201–204 (2005).
3. K. S. Novoselov, A. K. Geim, S. V. Morozov, D. Jiang, Y. Zhang, S. V. Dubonos, I. V. Grigorieva, A. A. Firsov, *Science*, **306**, 666–669 (2004).
4. K. S. Novoselov, E. McCann, S. V. Morozov, V. I. Fal'ko, M. I. Katsnelson, U. Zeitler, D. Jiang, F. Schedin, A. K. Geim, *Nature Phys*., **2**, 177–180 (2006).
5. N. M. R. Peres, F. Guinea, A. H. Castro Neto, *Phys. Rev. B*, **73**, 125411 (2006) .
6. P. R. Wallace, *Phys. Rev.*, **71**, 622 (1947).
7. A. K. Geim, K. S. Novoselov, *Nature Mater.*, **6**, 183–191 (2007).
8. D. Dorranian, E. Solati, L. Dejam, *Appl. Phys. A*, **109**, 307–314 (2012).
9. E. Solati, L. Dejam, D. Dorranian, *Opt. Laser Technol.*, **58**, 26–32 (2014).
10. E. Solati, M. Mashayekh, D. Dorranian, *Appl. Phys. A*, **112**, 689–694 (2013).
11. E. Solati, D. Dorranian, *J. Clust. Sci.*, **26**, 727–742 (2015).
12. A. Mehrani, D. Dorranian, E. Solati, *J. Clust. Sci.*, **26**, 1743–1754 (2015).
13. M. Moradi, E. Solati, S. Darvishi, D. Dorranian, *J. Clust. Sci*., **27**, 127–138 (2016).
14. A. Zamiranvari, E. Solati, D. Dorranian, *Opt. Laser Technol.*, **97**, 209–218 (2017).
15. E. Solati, D. Dorranian, *Bull. Mater. Sci.*, **39**, 1677–1684 (2016).
16. E. Solati, D. Dorranian, *J. Appl.Spectrosc.*, **84**, 490–497 (2017).
17. S. Z. Mortazavi, P. Parvin, A. Reyhani, *Laser Phys. Lett.*, **9**, 547–552 (2012).
18. G. X. Chen, M. H. Hong, L. S. Tan, T. C. Chong, H. I. Elim, W. Z. Chen, W. Ji, *J. Phys.: Conf. Ser.*, **59**, 289–292 (2007).
19. E. Solati, D. Dorranian, *Appl. Phys. B*, **122**, 76–86 (2016).
20. N. Tabatabaie, D. Dorranian, *Appl. Phys. A*, **122**, 558 (2016).
21. J. L. Chen, X. P. Yan, *J. Mater. Chem.*, **20**, 4328–4332 (2010).
22. V. Kumar, V. Singh, S. Umrao, V. Parashar, Sh. Abraham, A. K. Singh, G. Nath, P. S. Saxena, A. Srivastava, *RSC Adv.*, **4**, 21101–21107 (2014).
23. F. Y. Ban1, S. R. Majid, N. M. Huang, H. N. Lim, *Int. J. Electrochem. Sci.*, **7**, 4345–4351 (2012).
24. B. Pan, J. Xiao, J. Li, P. Liu, Ch. Wang, G. Yang, *Sci. Adv.*, **1**, e1500857 (2015).
25. R. M. Nikonova, M. A. Merzlyakova, V. I. Lad'yanov, V. V. Aksenova, *Inorg. Mater.: Appl. Res.*, **3**, 44–47 (2012).
26. A. C. Ferrari, *Solid State Commun.*, **143**, 47–57 (2007).
27. D. Graf, F. Molitor, K. Ensslin, C. Stampfer, A. Jungen, C. Hierold, L. Wirtz, *Nano Lett.*, **7**, 238–242 (2007).
28. L. Shahriary, A. A. Athawale, *Int. J. Renew. Energy Environ. Eng.*, **2**, 58–63 (2014).
29. K. N. Kudin, B. Ozbas, H. C. Schniepp, R. K. Prud'homme, A. Aksay, R. Car, *Nano Lett.*, **8**, 36–41 (2008).